First-Principles Non-Equilibrium Dynamic Modelling of Agitated Thin-Film Evaporators

Francesco Rossi[a], Michele Corbetta[a], Daniela Geraci[a], Carlo Pirola[b], Flavio Manenti*[a]

[a]Dipartimento di Chimica, Materiali e Ingegneria Chimica "Giulio Natta", Politecnico di Milano, Piazza Leonardo da Vinci 32, 20131 Milano, Italy
[b]Dipartimento di Chimica, Università degli Studi di Milano, Via Golgi 19, 20131 Milano, Italy
flavio.manenti@polimi.it

Agitated Thin-Film Evaporators (ATFE) are frequently employed in the industrial practice for instance they found important applications in pharmaceuticals, pulp & paper, bio-based chemicals production and food industry. They are characterized by the possibility to process high viscosity liquids or liquids with suspended solid particles exploiting the mixing turbulence realized by the impeller. These features allow, for instance, to recover light heat sensitive compounds from high-boiling viscous liquids or to strip volatiles from a product up to residual traces. Their performance and optimal design is significantly influenced by blades number, impeller speed, heating policy and changes in the inlet mixture composition. The latter is a quite common issue, especially in the food and biotech industry. This paper deals with the development of a first-principles non-equilibrium evaporator dynamic model that is able to predict the influence of the key operating conditions and boundary conditions on the evaporator performance. The adopted modelling strategy implies the use of the finite volumes method, by discretising the evaporator into several slices that are modelled as two-phase pseudo-CSTRs. Moreover, heat and mass transfer are considered with the use of suitable correlations. Finally, a case study, based on the ATFE for sugar aqueous solution concentration, is used to test the model.

1. Introduction

Agitated Thin-Film Evaporators (ATFE), also known as Wiped Film Evaporators (WFE) are often used to purify liquids with viscosities up to about 100 poise, to separate thermolabile mixtures, or in general, to provide short residence times in heated zones. ATFE are designed with a cylindrical shape and with an internal rotor that is used to spread a thin layer of liquid film on the inner side of a metallic wall, while a utility stream (e.g. steam or hot oil) provides heat flowing in the external jacket. The peculiarity of this unit operation is not the thin-film itself, also present in Falling Film Evaporators (FFE), but rather the mechanical wiping device that produces and agitates the liquid film (Mutzenburg, 1965). This mechanical concept permits the processing of high-viscosity liquids, liquids with suspended solids, or situations requiring liquid rates too small to keep the thermal surface of a falling-film evaporator uniformly wet, preventing surface starving and temperature hot spots. The ATFE achieves the contact between a downward liquid film and an uprising vapour flow in a counter current configuration (Figure 1). The mixing in the liquid phase is assured by the blades that during their rotation produce a thin-film and a bow wave in front of the blade where the excess liquid is directed and mixed. ATFE are widely used in the food, pulp & paper (Leite et al., 2014), pharmaceutical and biobased industry as concentrators and separators (Chawankul et al., 2003) due to their short residence times and relatively high heat transfer coefficients. In this work, a dynamic model is developed to study the influence of operating parameters (Komesu et al., 2014) and boundary conditions on the evaporator efficiency. Heat and mass transfer mechanisms involved in wiped film evaporators are strongly correlated with the blades geometry and are here described by means of semi-empirical correlations that account for these effects. In this way, the model provides a useful tool to optimize also the geometrical design of the evaporator rather than simply the operating parameters.

2. Dynamic model

With respect to conventional models with a steady-state formulation proposed in literature (Chawankul et al., 2003), this dynamic model is able to cope with start-up transients and changes in boundary conditions (e.g. feedstock variation). This last point is especially important for the biobased industry, where fluctuations of the feedstock are frequent. Moreover, there is no thermal equilibrium between the vapour and the liquid phases in each axial volume element (i.e. enthalpy balances are solved both for the liquid and vapour phases) as usually assumed. This is especially true at the inlet of the evaporator where the liquid film is contacted with the hot upraising vapour flowrate.

The stage-wise model is based on the main assumptions discussed below.

1. The mixing in each stage is approximated by that of a CSTR due to the action of the blades (i.e. the blades perfectly mix the solution in the bow wave and in the film underneath it of each stage).
2. It is assumed no backmixing along the evaporator.
3. The variables (concentration, temperature and speed) entering a stage are equal to those leaving the previous stage.
4. Since the film is very thin with respect to the diameter of the ATFE, a flat plate approximation can be used for diffusion.
5. The interface concentration of volatile species is the equilibrium concentration corresponding to the operating condition in the device.
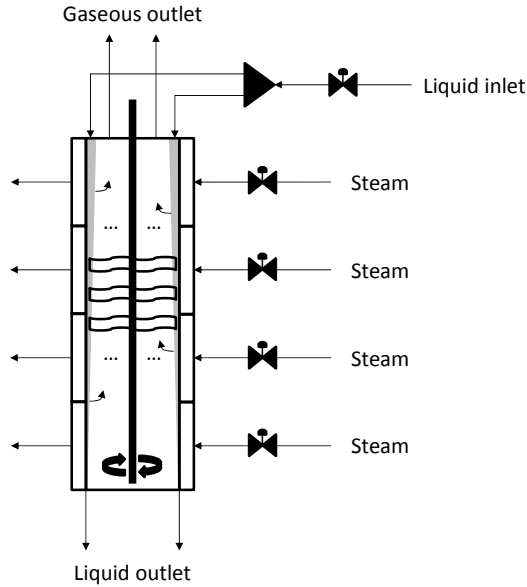6. The vapour phase is considered pseudo-stationary due to its fast dynamic response.

Figure 1: Schematic of the ATFE with inlet and outlet streams.

2.1 Balance equations

Considering the hypothesis discussed above, material energy and momentum balances are derived for both the vapour and the liquid phase as follows, where index i stands for the i-th species, n for the n-th stage, L and V for the liquid and vapour phase, ω is the mass fraction, ρ the density, A the cross-sectional area, v the velocity, J the mass transfer flux and V the volume.

$$\frac{d\omega_{i,n}^L}{dt} = \frac{\rho_{mix,n-1}^L A_{n-1}^L v_{n-1}^L}{\rho_{mix,n}^L V_n^L}\left(\omega_{i,n-1}^L - \omega_{i,n}^L\right) + \frac{A_n^{LV}}{\rho_{mix,n}^L V_n^L}\left(J_{i,n}^{LV} - \omega_{i,n}^L\sum_{i=1}^{NC} J_{i,n}^{LV}\right)$$

(0)

$$0 = \rho_{mix,n+1}^V A_{n+1}^V v_{n+1}^V \omega_{i,n+1}^V - \rho_{mix,n}^V A_n^V v_n^V \omega_{i,n}^V - A_n^{LV} J_{i,n}^{LV}$$

(0)

$$\frac{dV_n^L}{dt} = -\frac{V_n^L}{\rho_{mix,n}^L}\frac{d\rho_{mix,n}^L}{dt} + \frac{\rho_{mix,n-1}^L}{\rho_{mix,n}^L}A_{n-1}^L v_{n-1}^L - A_n^L v_n^L + \frac{A_n^{LV}}{\rho_{mix,n}^L}\sum_{i=1}^{NC}J_{i,n}^{LV} \tag{0}$$

$$0 = \rho_{mix,n+1}^V A_{n+1}^V v_{n+1}^V - \rho_{mix,n}^V A_n^V v_n^V - A_n^{LV}\sum_{i=1}^{NC}J_{i,n}^{LV} \tag{0}$$

$$0 = \rho_{mix,n}^L V_n^L g - \frac{1}{2}\rho_{mix,n}^L f_n^{LW} A^{LW}\left(v_n^L\right)^2 - \frac{1}{2}\rho_{mix,n}^V f_n^{LV} A^{LV}\left(v_n^V + v_n^L\right)^2 \tag{0}$$

Eq(1) is the liquid mass conservation of the i-th species within the n-th finite volume, Eq(2) is the vapour mass conservation of the i-th species within the n-th finite volume, Eq(3) and Eq(4) are the global material balances for the liquid and vapour phase respectively, while Eq(5) is the momentum balance for the n-th stage. Enthalpy balances are solved with a double regime model that considers evaporation for temperatures below the liquid bubble point and boiling when the liquid is at the bubble point for each n-th stage. In the latter case, the liquid temperature is fixed (i.e. the bubble temperature), and the enthalpy balance is used to calculate the total boiling vapour flux, whereas during evaporation, the material flux migrating in the vapour phase is determined by the mass transfer coefficient. During evaporation, Eq(6) and Eq(7) are considered. These equations are the liquid and vapour enthalpy balances respectively, where T is temperature, Cp the heat capacity, h the heat transfer coefficient, U the global heat transfer coefficient and Δh the heat of evaporation.

$$\frac{dT_n^L}{dt} = \frac{1}{\rho_{mix,n}^L V_n^L \sum_{i=1}^{NC}\omega_{i,n}^L c_{p_{i,n}}^L}\left[\rho_{mix,n-1}^L A_{n-1}^L v_{n-1}^L\left(T_{n-1}^L - T_n^L\right)\sum_{i=1}^{NC}\omega_{i,n-1}^L \frac{c_{p_{i,n-1}}^L + c_{p_{i,n}}^L}{2} + \right.$$
$$\left. + A_n^{LV}\sum_{i=1}^{NC}J_{i,n}^{LV}\frac{c_{p_{i,n}}^L\left(T_n^L\right) + c_{p_{i,n}}^L\left(T_n^V\right)}{2}\left(T_n^V - T_n^L\right) + A_n^{LV}h_n^{LV}\left(T_n^V - T_n^L\right) + A^{LW}U_n^{LW}\left(T_{steam} - T_n^L\right)\right] \tag{0}$$

$$0 = \rho_{mix,n+1}^V A_{n+1}^V v_{n+1}^V\left(T_{n+1}^V - T_n^V\right)\sum_{i=1}^{NC}\omega_{i,n+1}^V\frac{c_{p_{i,n+1}}^V + c_{p_{i,n}}^V}{2} +$$
$$- A_n^{LV}\sum_{i=1}^{NC}J_{i,n}^{LV}\frac{c_{p_{i,n}}^L\left(T_n^L\right) + c_{p_{i,n}}^L\left(T_n^V\right)}{2}\left(T_n^V - T_n^L\right) - A_n^{LV}h_n^{LV}\left(T_n^V - T_n^L\right) \tag{0}$$

During boiling, Eq(8) and Eq(9) are considered. These equations are the liquid and vapour enthalpy balances respectively.

$$0 = \frac{1}{\rho_{mix,n}^L V_n^L \sum_{i=1}^{NC}\omega_{i,n}^L c_{p_{i,n}}^L}\left[\rho_{mix,n-1}^L A_{n-1}^L v_{n-1}^L\left(T_{n-1}^L - T_n^L\right)\sum_{i=1}^{NC}\omega_{i,n-1}^L\frac{c_{p_{i,n-1}}^L + c_{p_{i,n}}^L}{2} + \right.$$
$$\left. + A_n^{LV}J_n^{TOT}\sum_{i=1}^{NC}\omega_{i,n}^{V,eq}\Delta h_{i,n}^{ev}\left(T_n^L\right) + A_n^{LV}h_n^{LV}\left(T_n^V - T_n^L\right) + A^{LW}U_n^{LW}\left(T_{steam} - T_n^L\right)\right] \tag{0}$$

$$0 = \rho_{mix,n+1}^V A_{n+1}^V v_{n+1}^V\left(T_{n+1}^V - T_n^V\right)\sum_{i=1}^{NC}\omega_{i,n+1}^V\frac{c_{p_{i,n+1}}^V + c_{p_{i,n}}^V}{2} +$$
$$- A_n^{LV}J_n^{TOT}\sum_{i=1}^{NC}\omega_{i,n}^{V,eq}\Delta h_{i,n}^{ev}\left(T_n^L\right) - A_n^{LV}h_n^{LV}\left(T_n^V - T_n^L\right) \tag{0}$$

2.2 Closure equations and correlations

The mathematical model requires the definition of transport coefficients (heat, mass and momentum) and a vapour-liquid equilibrium model in order to be solved. The latter is used to define both the composition of the evaporating flux in equilibrium with the liquid film and to check the bubble temperature of the liquid mixture in each finite volume, in order to choice between the evaporative or the boiling models. On the other hand, suitable correlations should be used to evaluate transport coefficients accounting for the effect of the number of blades, the rotational velocity and evaporator geometry. The global heat transfer coefficient is calculated by considering a series of thermal resistances that are related to the internal heat transfer, the metallic wall conduction and the external heat transfer within the heating jacket, and it is evaluated with Eq(10). For the external heat transfer, the Nusselt theory for film condensation on vertical tubes is assumed (Eq(11)), whereas for internal heat transfer the correlation by Bott and Romero (Bott and Romero, 1963) is considered (Eq(12)). It is important to highlight that the Nusselt number for internal heat transfer is correlated to the number of blades (N_b) and to the rotational Reynolds number (Re_N), depending on the blades speed.

$$\frac{1}{U_i} = \frac{1}{h_i} + \frac{D_i}{2\lambda_{wall}} \ln\left(\frac{D_e}{D_i}\right) + \frac{D_i}{h_e D_e} \tag{1}$$

$$h_e = 0.925 \left(\frac{\lambda^3 \rho^2 g}{\mu \Gamma}\right)^{1/3} \tag{2}$$

$$Nu_D = \frac{h_i D_i}{\lambda} = 0.65 \, \mathrm{Re}_f^{0.25} \, \mathrm{Re}_N^{0.43} \, \mathrm{Pr}^{0.3} \, N_b^{0.33} \tag{3}$$

Mass transfer in ATFE has not been extensively addressed in technical literature. For this reason, in this work, the analogy for heat and mass transfer mechanisms is used. Heat transfer correlations are available for both FFE and ATFE and mass transfer correlations are available only for FFE. Introducing an heat transfer enhancing coefficient (β) for ATFE, the analogy allows to consider the same enhancing factor also for mass transfer (Eq(13)), leading to an estimation of the mass transfer coefficient for ATFE.

$$\beta = \frac{h_i^{ATFE}}{h_i^{FFE}} = \frac{K_c^{ATFE}}{K_c^{FFE}} \tag{4}$$

It is now possible to solve the differential algebraic system (DAE) by fixing initial conditions for the differential equations (composition, temperature and flowrate of the liquid within the evaporator) and boundary conditions at the inlet and outlet of the evaporator. The resulting DAE system has a jacobian matrix sparsity pattern outlined in Figure 2, where in the central blocks non-zero elements are highlighted, and it is solved with the BzzMath numerical library (Buzzi-Ferraris and Manenti, 2012), based on the Gear multivalue method.
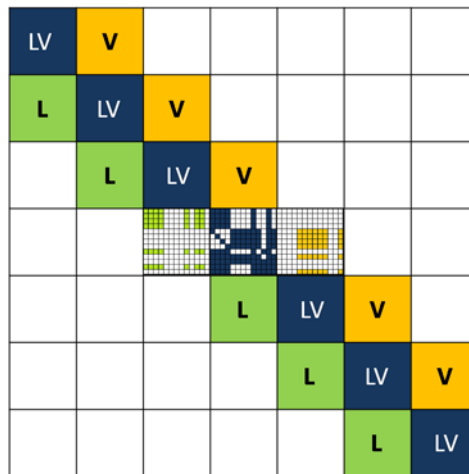

Figure 2: Jacobian matrix sparsity pattern.

3. Case study: evaporation of a sucrose aqueous solution

In order to test the model, a case study dealing with a sucrose aqueous solution concentration is here considered. Geometric and operating parameters used for the simulation are reported in **Errore. L'origine riferimento non è stata trovata.** and **Errore. L'origine riferimento non è stata trovata.**, respectively.
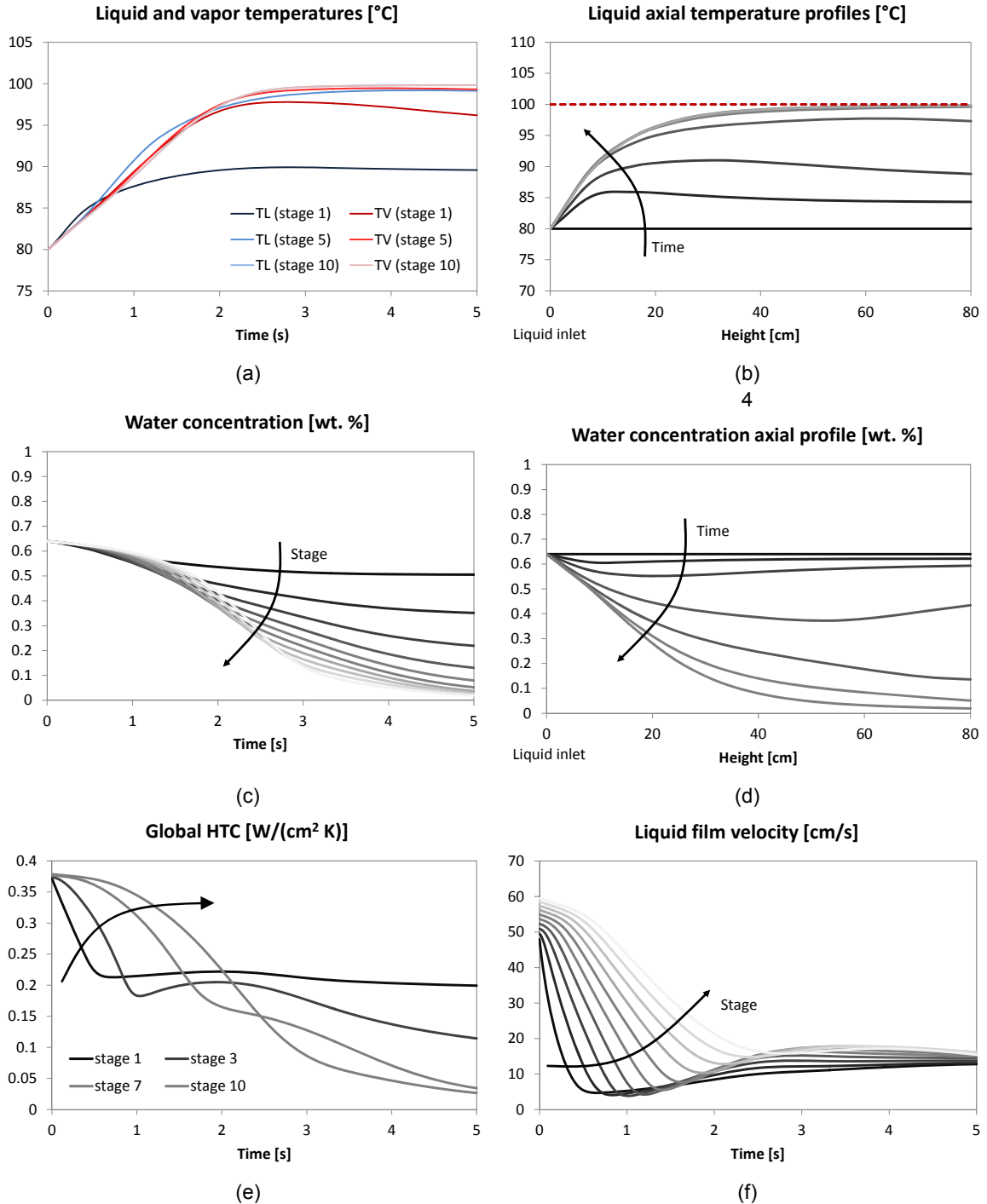

(a)

(b)

4

(c)

(d)

(e)

(f)

Figure 3: Model results of temperatures and species concentrations along the axial length and during time.

Figure 3 shows model results of temperatures and species concentrations along the axial length and during time, starting from an initial condition where the evaporator is at 80 °C and with a sucrose concentration of 36 wt. % in each volume element. Panel (a) shows liquid and vapour temperature dynamic evolution; panel (b) liquid temperature axial profiles at different times; panel (c) liquid composition dynamic evolution; panel (d) liquid

composition axial profiles; panel (e) the dynamic evolution of the global Heat Transfer Coefficient (HTC); and finally panel (f) shows vapour and liquid (film) velocities dynamic evolution.

Table 1: Geometric parameters of the evaporator used for the simulation

Parameter	UOM	Value
Internal diameter	[cm]	6
Evaporator length	[cm]	80
Wall thickness	[cm]	0.635
Clearance	[cm]	0.2
Number of blades	[-]	2

Table 2: Operating parameters used for the simulation

Parameter	UOM	Value
Pressure	[atm]	1
Steam temperature	[°C]	100
Steam flowrate	[kg/s]	0.0025
Liquid inlet flowrate	[kg/s]	0.02
Liquid inlet temperature	[°C]	80
Liquid inlet sucrose concentration	[wt. %]	36

4. Conclusions

This work proposes a comprehensive dynamic model of Agitated Thin-Film Evaporators (ATFE). This kind of unit operation has important features that allows to process heat sensitive materials with high heat transfer coefficients and low residence times.

The model is successfully applied to the case study of a sucrose aqueous solution concentration problem, highlighting the output that the model is able to produce. Further validation examples and comparisons with experimental data will be the object of future works.

The model provides a useful tool for the optimization of this kind of equipment in terms of both operating conditions and design variables, which will be the objective of future works.

References

Bott, T. R., Romero, J. J. B.,1963, Heat Transfer Across a Scrapped Surface, Canadian Journal of Chemical Engineering, 41, 213-219.

Buzzi-Ferraris, G., Manenti, F., 2012, BzzMath: Library Overview and Recent Advances in Numerical Methods, Computer Aided Chemical Engineering, 30, 1312-1316.

Chawankul N., Chuaprasert S., Douglas P., Luewisutthichat W., 2003, Optimisation of an Agitated Thin Film Evaporator for Concentrating Orange Juice Using AspenPlus, Developments in Chemical Engineering & Mineral Processing, 11, 309-322.

Komesu A., Martins P., Oliveira J., Lunelli B.H., Maciel Filho R., Wolf Maciel M.R., 2014, Purification of lactic acid produced from sugarcane molasses, Chemical Engineering Transactions, 37, 367-372 DOI: 10.3303/CET1437062.

Leite B.S., Andreuccetti M.T., Leite S.A.F., d´Angelo J.V.H., 2014, Study of sodium salts solubility in eucalyptus black liquor to understand and prevent scale formation in evaporators, Chemical Engineering Transactions, 39, 451-456 DOI:10.3303/CET1439076.

Mutzenburg A. B., 1965, Agitated Thin-Film Evaporators. Part 1. Thin-Film Technology, Chemical Engineering,, 72(19), 175-178.